JES Focus Issue of Selected Papers from IMLB 2018

Analysis of Degradation of Si/Carbon||$LiNi_{0.5}Mn_{0.3}Co_{0.2}O_2$ Full Cells: Effect of Prelithiation

Arlavinda Rezqita,[z] Anish-Raj Kathribail, Jürgen Kahr, and Marcus Jahn

AIT Austrian Institute of Technology GmbH, Center for Low-Emission Transport, 1210 Vienna, Austria

Despite considerable progress of silicon/carbon (Si/C) composites anodes, they still suffer from high irreversible capacity losses, which are mainly due to continuous Solid Electrolyte Interphase (SEI) layer formation, which consumes a large amount of lithium. To compensate for the active lithium losses, prelithiation of Si-based anodes has been attempted. In this manuscript, we report the effect of prelithiation on Si/C anodes combined with $LiNi_{0.5}Mn_{0.3}Co_{0.2}O_2$ cathodes in full cell configurations. To prepare Li_xSi/C anodes, Si/C electrodes were lithiated electrochemically at 0.1 and 0.5 V vs. Li/Li^+ in half cell configuration before assembly of the full cell. Special attention is paid to the effect of the degree of prelithiation on initial electrochemical behavior and Li dendrite formation. In this work, electrochemical investigations were performed by using two-electrode and three-electrode measurements. Furthermore, the morphology of the active materials before and after cycling were characterized by post mortem Scanning Electron Microscopy (SEM).

 [DOI: 10.1149/2.0671903jes]

Manuscript submitted October 26, 2018; revised manuscript received December 25, 2018. Published February 2, 2019. *This paper is part of the JES Focus Issue of Selected Papers from IMLB 2018.*

Graphitic carbon is the conventional standard material for the negative electrode of Li-ion batteries. However, graphite has a relatively low theoretical charge capacity of 372 mAh g^{-1}, which is due to lithium storage via formation of LiC_6, and also experiences capacity fading at high charge and discharge rates.[1] Silicon (Si) is seen as one of the most promising anode materials for the next-generation high energy Li-ion batteries due to its theoretical capacity of 3579 mAh g^{-1} (based on $Li_{15}Si_4$) and a low electrochemical potential (between 0.37 and 0.45 V versus Li/Li^+) which is beneficial for active materials for anodes;[2] it is also the second most abundant element on earth. A further key advantage of Si is its high volumetric capacity (8303 mAh cm^{-3}), an important feature wherever space for the battery is at a premium. However, the main shortcomings of Si anodes are the volume changes (280–400%) during lithiation/delithiation which lead to progressive pulverization and electric contact loss, causing capacity fading as well as potentially catastrophic failure. Furthermore, it is subject to high irreversible capacity losses during the first charge-discharge cycles.[3] Although volume expansion can be minimized by the use of nanostructured Si or limiting its capacity and conductivity can be improved by the addition of conductive additives, some issues related to high irreversible capacity losses still remain due to continuous Solid Electrolyte Interphase (SEI) layer formation, which consumes a large amount of lithium.[4,5] In order to compensate for active lithium losses during SEI formation, various prelithiation techniques such as (1) chemical lithiation using active reactants, (2) electrochemical prelithiation, (3) direct contact to lithium metal, and (4) utilization of lithiated active materials have been attempted and comprehensively reviewed by Holtstiege *et al.*[6] In the case of Si, prelithiation has an additional advantage, since after first delithiation, void spaces are generated which can buffer the volume expansion of Si during cycling, resulting in improved electrochemical performance stability.[7] For Si,[8] Si nanowires-carbon,[9,10], Si/C composites,[9–11] Si/graphene oxide composites,[12] either electrochemical prelithiation techniques or direct contact to lithium metal have been attempted. In these studies, prelithiation was shown to be a promising approach to compensating for the active lithium loss during the 1st cycle, which is attributed mainly to SEI formation. However, the degree of prelithiation needs to be carefully controlled since overlithiation can lead to lithium plating and short circuits, while insufficient lithiation leaves Li trapping sites and does not improve the initial Coulombic efficiency enough. Kim et al. introduced prelithiation of SiO_x electrodes based on electrically shorting them with lithium metal foil, and suggested a point where the final voltage is below that which is necessary for SEI layer formation, but above that alloying reaction.[13] However, previous studies have not yet answered the question at which point lithium plating occurs in these prelithiated materials.

On the cathode side, high nickel content $Li_1Ni_{0.5}Mn_{0.3}Co_{0.2}O_2$ (NMC532) is a promising cathode material for electric vehicles due to its high energy density[14] and rate capability.[15] In this work, we aim to study the effect of the degree of prelithiation on the initial electrochemical behavior of Li-ion cells containing a Si/C anode and a $LiNi_{0.5}Mn_{0.3}Co_{0.2}O_2$ cathode by using two-electrode and three-electrode cells. The three-electrode cell enables monitoring both the potentials of the anode and cathode vs. Li and their potential against each other in a full cell. None of the previous works on prelithiated Si/C composites monitored the degree of lithiation in this way. Results from these studies could provide significant insights into the long-term performance of the full cells containing Si-based anodes.

Experimental

Si/C composites were synthesized by dispersing Si nanoparticles (30–50 nm, Nanostructured and Amorphous Materials, Inc.) in a phenolic resin, then carbonizing at 650°C in an Argon atmosphere for 10 h. The mixture of the synthesized Si/C composites (75 wt%), Super C45 (Timcal, 15 wt%), polyacrylic acid (PAA, Fluka, 10 wt%) in an N-methyl-2-pyrrolidone (NMP, Sigma Aldrich) solvent was used for preparing negative electrode materials. The anodes have coating thickness of 0.032 mm and the total coating loading: 0.55 mg/cm^2. To combine the negative electrode for a full cell configuration, $LiNi_{0.5}Mn_{0.3}Co_{0.2}O_2$ (NMC532, BASF) was used as active material for the positive electrode. The NMC532 positive electrode was prepared by mixing NMC532 (84 wt%), Super C65 (Timcal, 6 wt%), conductive graphite (2 wt%), and polyvinylidene fluoride (PVDF, Solvay, 8 wt%). The cathodes have coating thickness of 0.050 mm and the total coating loading: 2.85 mg/cm^2. 1M $LiPF_6$ in ethylene carbonate: ethyl methyl carbonate (EC: EMC) = 3:7 wt/wt% + 2 wt% VC (SoulBrain MI) was used as electrolyte. Celgard 2325 (PP/PE/PP) was used as separator. To prepare Li_xSi/C anodes, Si/C electrodes were lithiated electrochemically by using an EL Cell at a C-rate of C/20 with galvanostatic mode at 0.1 and 0.5 V vs. Li/Li^+ in half cell configuration before assembly of the full cell. Afterwards, non-prelithiated and prelithiated Si/C (Li_xSi/C) anodes were combined with NMC532 cathodes in CR 2032 type coin cells. For cell balancing, the practical

[z]E-mail: arlavinda.rezqita@ait.ac.at

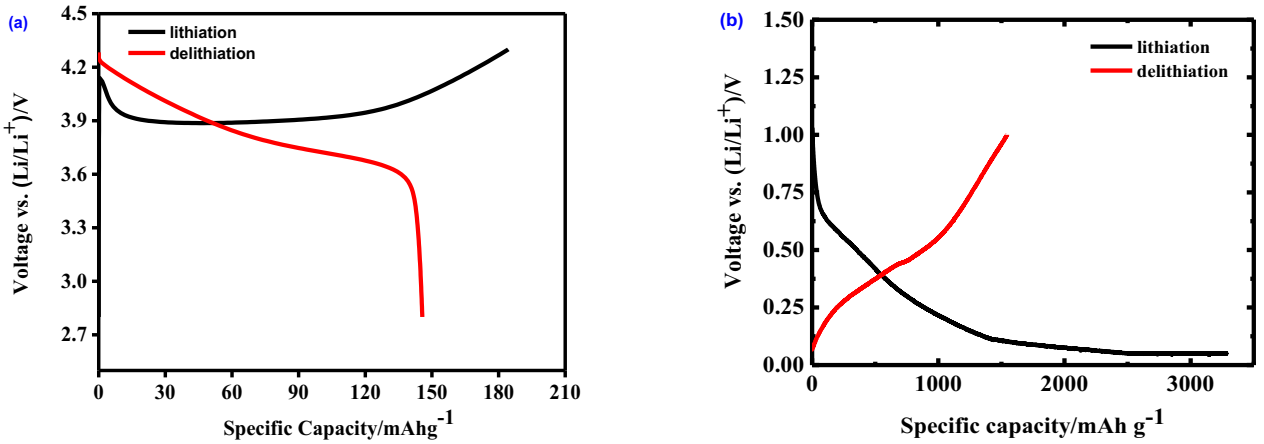

Figure 1. (a) 1st cycle of voltage vs. specific capacity profiles of NMC532 vs. Li cell cycled in the potential range of 2.8–4.3 V vs. Li/Li^+; (b) Si/C vs. Li cell cycled in the potential range of 0.05–1 vs. Li/Li^+.

areal capacity ratio of the pristine anode and cathode (N:P) was designed to be 1.3: 1, which was calculated based on the anode potential range of 0.05–1 V vs. Li/Li^+. The C-rate was calculated based on the practical capacity of the NMC532 (mAh g^{-1}). The cells were cycled in a Maccor series 4000 with the cut-off voltages of 3–4.2 V.

The three-electrode measurement was performed in Swagelok-T-cells, using an NMC532 cathode as working electrode, a Si/C anode as counter electrode, and metallic lithium foil as reference electrode, as described in detail by Ender et al.[16] The three-electrode cells were cycled with Galvanostatic Cycling with Potential Limitation (GCPL) technique in Biologic VMP3 instruments. The two-electrode CR 2032 type coin cells were cycled in a Maccor Series 4000 battery tester. All electrochemical measurements were performed at room temperature. The cut-off cell voltages were 3–4.2 V and the C-rate was set to 0.1 C. Electrodes of 15 mm and 10 mm diameters were tested for a two- and three- electrode configuration, respectively. SEM analysis was conducted by FEI/Philips XL-30 Field Emission ESEM coupled with an Energy Dispersive X-ray spectroscopy (EDX) at a working distance of 10 mm and an accelerating voltage of 30 keV. The sample were exposed to air before SEM and EDX analysis.

Results and Discussion

Initial electrochemical performance in half cells.—Figure 1 shows 1st cycle potential vs. specific capacity profiles of NMC532 (a) and Si/C (b) vs. Li cell in a half cell configuration. The NMC532 potential profiles show distinct slopes with an initial discharge capacity of 150 mAh g^{-1} and Coulombic efficiency of 78.8% in the potential range of 2.8–4.3 V vs. Li/Li^+. During lithium extraction, Ni^{2+} is oxidized to Ni^{3+} and Ni^{4+}. The polarization during the 1st charge can be attributed to the hydroxides from the reaction of the NMC surface with humidity and the carbonates from the reaction of CO_2 with humidity, which were also observed on Ni-rich NMC materials when the electrodes were stored under ambient air.[17] The Si/C electrode exhibits an initial discharge capacity of 3909 mAh g^{-1} and Coulombic efficiency of 44.6% in the potential range of 0.05 - 1 vs. Li/Li^+. Note that a very high irreversible capacity loss is attributed to the high specific surface areas of the Si/C composites (526.32 m^2g^{-1}) which leads to decomposition of a large amount of electrolyte.

Electrochemical performance in full cells.—Furthermore, Si/C anodes and NMC cathodes were combined and tested in a two-electrode set-up cell. Figure 2a shows 1st and 2nd cycle potential vs. capacity profiles (E vs. Q) of the full cells prepared from non-prelithiated Si/C. In the first cycle, the non- prelithiated cell exhibits an initial charge capacity of 212 mAh g^{-1}; however, after the 1st formation cycle, the cell shows a discharge capacity of 48 mAh g^{-1} (initial Coulombic efficiency: 25%) due to SEI formation. In contrast, a Si/C anode, prelithiated at 100 mV (shown in Figure 2b) showed a superior electrochemical performance. While the prelithiated cell delivered a specific charge capacity of 160 $mAhg^{-1}$ in the first cycle, initial capacity loss was significantly reduced (initial Coulombic efficiency: 86%).

Furthermore, the electrochemical behavior of the Si/C anodes with different degrees of prelithiation (prelithiated at different voltages vs. Li/Li^+) in the full cells was also assessed. To investigate cell

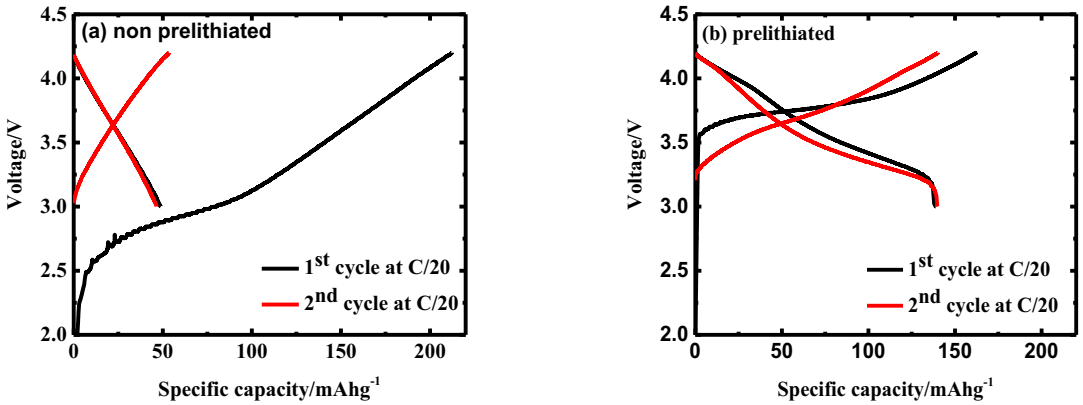

Figure 2. Voltage vs. specific capacity profiles of the full cell containing (a) non-prelithiated Si/C and (b) prelithiated Si/C anode at 0.1 V, each coupled with an NMC cathode.

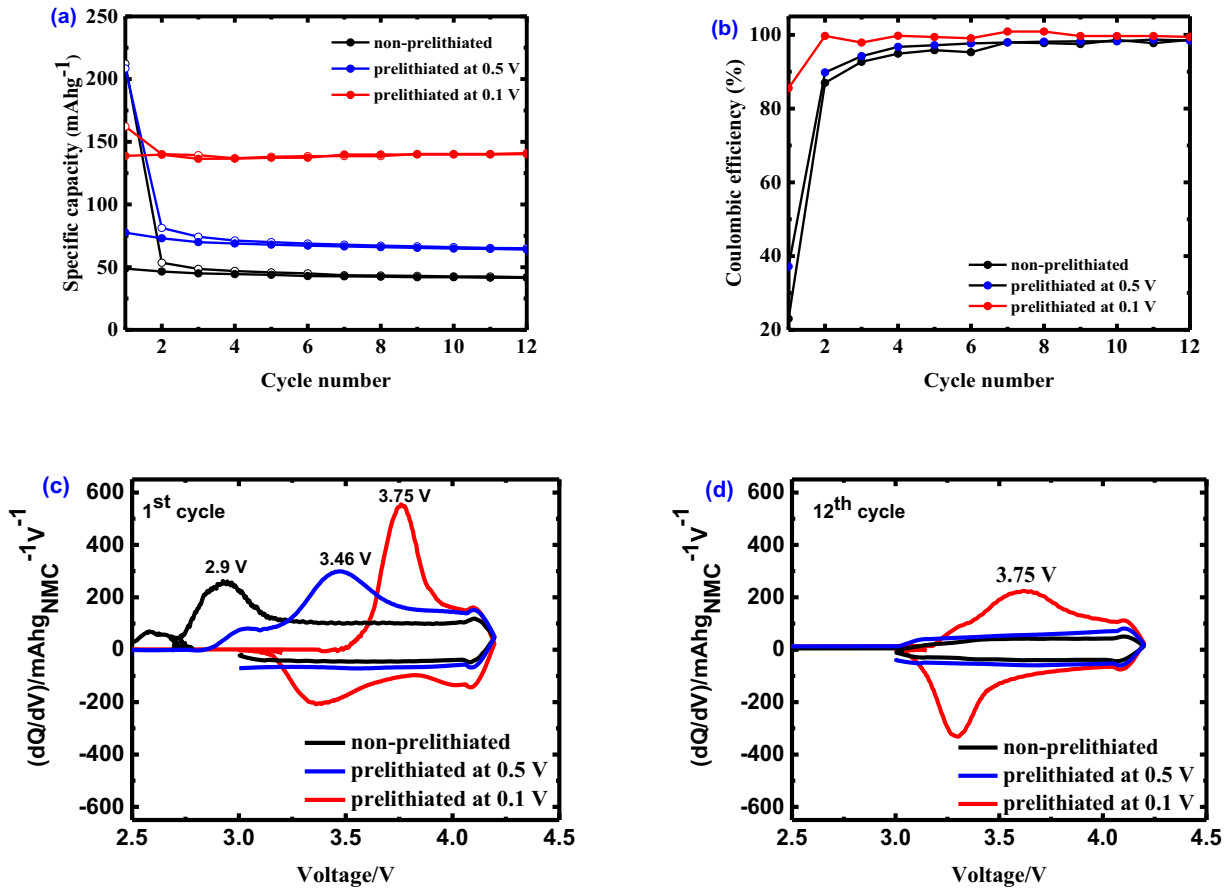

Figure 3. (a) Specific capacity and (b) coulombic efficiency vs cycle number profiles, dQ/dV vs. voltage profiles of (c) the 1st cycle and (d) the 12th cycle of the full cells containing NMC532 cathodes with Si/C anodes with different degrees of prelithiation in two-electrode set-up.

degradation, Coulombic efficiency was calculated. Specific capacity and Coulombic efficiency profiles of the cells in the first few cycles of the cells containing non-prelithiated Si/C, Si/C prelithiated at 0.5 V, and Si/C prelithiated at 0.1 V can be seen in Figures 3a and 3b. The cell with the non-prelithiated anode exhibits an initial charge capacity of 212 mAh g^{-1}; however, after 12 cycles there is poor electrochemical performance with a discharge capacity of 41 mAh g^{-1} and a Coulombic efficiency of 98.66%. On the other hand, those with prelithiated Si/C anodes show an improvement (discharge capacity of 64 $mAhg^{-1}$, Coulombic efficiency of 98% for a prelithiated cell at 0.5 V, and discharge capacity of 140 $mAhg^{-1}$, Coulombic efficiency of 99.45% for prelithiated cell at 0.1 V).

To determine the changes in the negative and positive electrode peaks or the relative electrode slippages, dQ/dV analyses were performed for the 1st and 12th cycle, shown in Figures 3c and 3d. Although it is difficult to distinguish the contributions of each electrode from the dQ/dV plots, the distinguishable features such as the changes in peak position and the peak width can give us valuable information regarding parasitic reactions and material loss.[18] The peaks in the dQ/dV curves are derived from pseudo-phase equilibria (i.e., polarization).[19] In the 1st cycle, during lithiation the cell with a non-prelithiated anode shows an oxidation peak at 2.6 V which does not appear in the prelithiated samples. This peak could be attributed to SEI layer formation. An oxidation peak at 2.9 V is observed for the non-prelithiated cell, which is shifted to 3.46 V and 3.75 V for prelithiated cells at 0.5 V and 0.1 V, respectively. Based on Ohm's law (V = I * R), we can assume that the shifts in peak position (potential) indicate increases in internal resistance, while the widening of peaks points to chemical changes to the electrode materials. After 12 cycles, these peaks weaken, especially for the non-prelithiated sample and for the one prelithiated at 0.5 V. On the other hand, the sample prelithiated at 0.1 V maintains the oxidation and reduction peaks at 3.75 V and 3.3 V, respectively, showing the electroactivity of both electrodes.

Three-electrode set-up measurement.—To monitor the potential of the anodes and cathodes vs. Li as well as in full cells and to verify whether lithium plating occurred, three-electrode set-up cells were assembled. Figure 4 shows the voltage vs time profiles of the full cell, NMC532, and Si/C anodes (both non-prelithiated and prelithiated). While the full cell potential is fixed between cut off voltages (3–4.2 V), it becomes evident that the positive and negative electrode potentials shift to slightly higher values during cycling. Figure 5 shows in more detail the potential increases of NMC532 cathodes and Si/C anodes after charge and discharge for the 1st and 12th cycles. The increasing cut-off potentials at the endpoints of cell discharge are more pronounced for the cells containing non-prelithiated (shown in black) and prelithiated anodes at 0.5 V (shown in blue), indicating that capacity loss was experienced by both cells.[18,20] These increases are much less pronounced in the cell containing an anode prelithiated at 0.1 V (shown in red). This means that less shifts in the cathode and anode potentials take place during cycling, which might be attributed to the higher content of lithium. In addition, since Si has semiconductor properties, the electronic conductivity of Si anode generally increases with increased amount of conductive lithium.

Figure 6 depicts the closer look at voltage profiles of the Si/C anodes with different degrees of prelithiation for the 1st cycle (a) and for 10 cycles (b). To better see the plateaus, the dQ/dV profiles of the 1st cycle of the electrode non-prelithiated and prelithiated at 0.1V are given in Figure 6c and the electrode prelithiated at 0.5 V (d). A peak at ~0.7 V vs. Li/Li^+ in the non-prelithiated Si can be assigned to SEI layer formation. The reducing profile in the range of 400–50 mV vs. Li/Li^+ can be assigned to the Li alloying into the Si.[21] While,

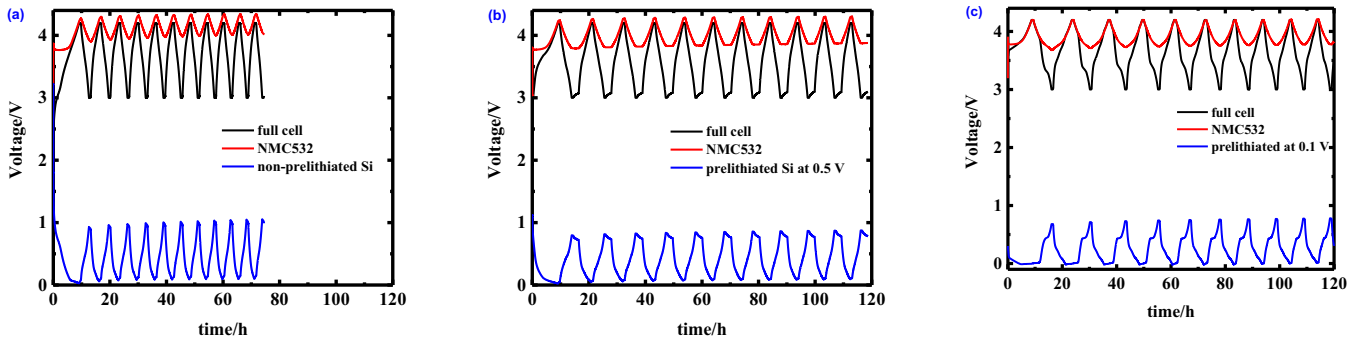

Figure 4. Voltage profiles of the overall experiment for the non-prelithiated (a) prelithiated at 0.5 V (b) prelithiated at 0.1 V (c). The red line corresponds to the positive half cell (NMC532), the blue one corresponds to the negative half cell (Si/C), and the black line to the full cell voltages.

the electrode prelithiated at 0.5 V shows a reduction peak at 0.45 V. Distinguished peaks for different degrees of prelithiation indicate a different mechanism for further Li de-/insertion during cycling.

Special attention is paid to the lithium deposition/plating which can lead to both safety issues and rapid performance degradation.[22] Li plating can thermodynamically occur as soon as the negative electrode potential is lower than or equal to the equilibrium potential $E_{Li^+/Li}$.[23] From Figure 6, it is evident that Li deposition occurs at the anode which was prelithiated at 0.1 V vs. Li/Li$^+$. Electrode balancing, which is expressed as the negative/positive (N/P) ratio, is an important factor influencing Li deposition on the cell level.[24] Prelithiation in the negative anode leads to lower N/P, thus it becomes more prone to Li deposition. Moreover, on the atomic level, Li deposition is affected by temperature and charging C-rate.[25]

From Figure 6b it can be seen that the cut-off potential increases strongly in the non-prelithiated anode, which is a sign of Li loss. It is worth mentioning that there is no lithium plating on the non-prelithiated and prelithiated Si/C at 0.5 V vs. Li/Li$^+$. It seems that the Si/C prelithiated at 0.5 V vs Li/Li$^+$ is a good compromise to add more Li after SEI formation without causing Li plating during cycling in in the full cell configuration.

Post mortem SEM and EDX analysis.—SEM was performed on both the pristine and the cycled Si/C electrodes to investigate any changes in the morphology of the particles during cycling. Figure 7 shows SEM images of the pristine Si/C electrode (a), and of the cycled Si/C electrodes which were non-prelithiated (b), prelithiated at 0.5 V (c), and prelithiated at 0.1 V (d). The SEM image of the pristine electrode shows an uneven and rough surface composed of Si nanoparticles, amorphous carbon, and carbon black. A similar morphology can be seen on the non-prelithiated electrode after cycling. While, those which are prelithiated show agglomeration and some polymeric-like films covered on the surface which can be assigned to electrolyte decomposition products. These were confirmed from the EDX data, in which a significant amount of anion decomposition species seems to be deposited on the surface. It is worth mentioning that the electrode prelithiated at 0.1V shows some whiskers/needle-like shapes, which lead us to believe that Li dendrites were beginning to form Refs. 26,27. This confirms Li dendrite growth on the Si/C prelithiated at 0.1 V, which was also indicated from the 3-electrode measurement set-up.

Furthermore, elemental mapping of the pristine and cycled electrodes was done by using EDX analysis and quantitative analysis, as summarized in Table I. The analyses indicate that the pristine electrode contains Si, C, and Cu, originating from the active materials and the current collector. The cycled electrodes show O, F, P, which are derived from the decomposition of the electrolyte. Li is unfortunately not detectable by EDX analysis. However, we can point out that the electrode prelithiated at 0.1V shows a much higher oxygen content which can be assigned to Li_2O. The O atom can also be derived from the the polymeric layer and Li_2CO_3 in the SEI film, however F and P are shown much less in the prelithiated anode at 0.1 V.

Conclusions

In this work, we investigated the initial cycling performance of NMC532‖Si/C full cells, particularly the effect of the prelithiation of Si/C anodes. The two-electrode set-up measurements showed that the cell with Si/C prelithiated at 0.1 V vs. Li/Li$^+$ exhibited a significantly higher initial Coulombic efficiency in comparison to the

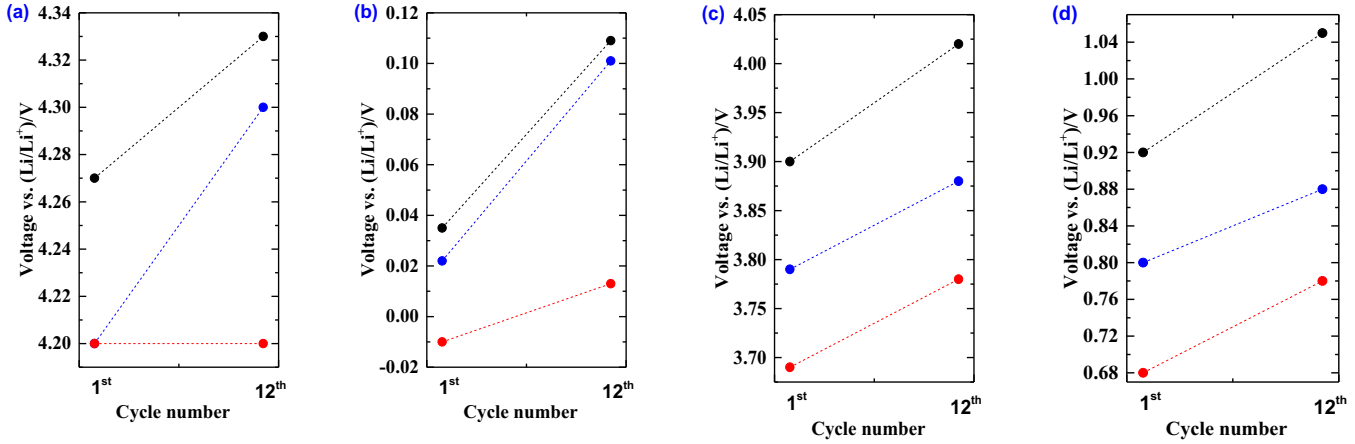

Figure 5. (a) Voltage of NCM523 electrodes after cell charge, (b) Si/C electrodes after cell charge, (c) NCM523 electrodes after cell discharge, and (d) Si/C electrodes after cell discharge. The cells containing non-prelithiated Si/C, prelithiated at 0.5 V, and prelithiated at 0.1 V are shown in black, blue and red, respectively.

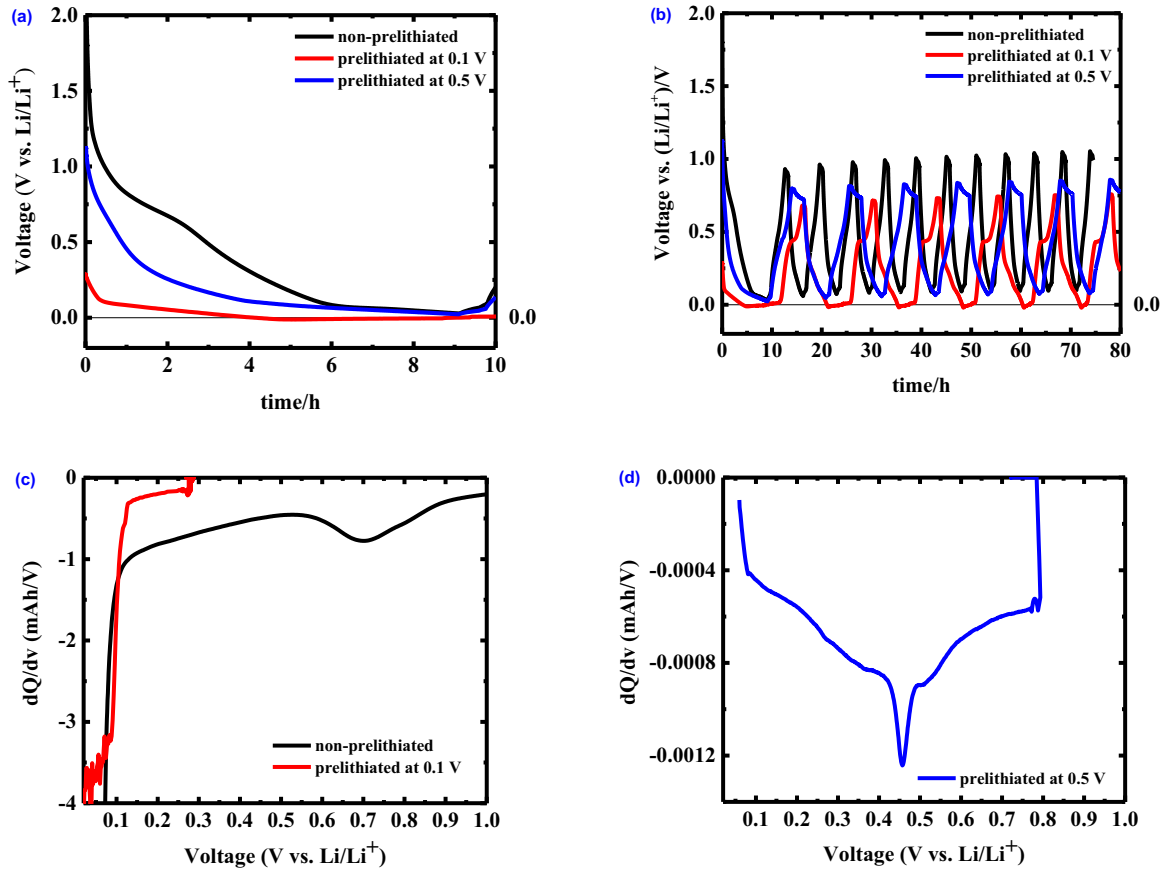

Figure 6. Voltage profiles of the Si/C anodes with different degrees of prelithiation for (a) 1st cycle, and (b) 10 cycles, dQ/dV vs. voltage profiles of the 1st cycle of (c) the non prelithiated and prelithiated at 0.1 V and (d) the prelithiated at 0.5 V.

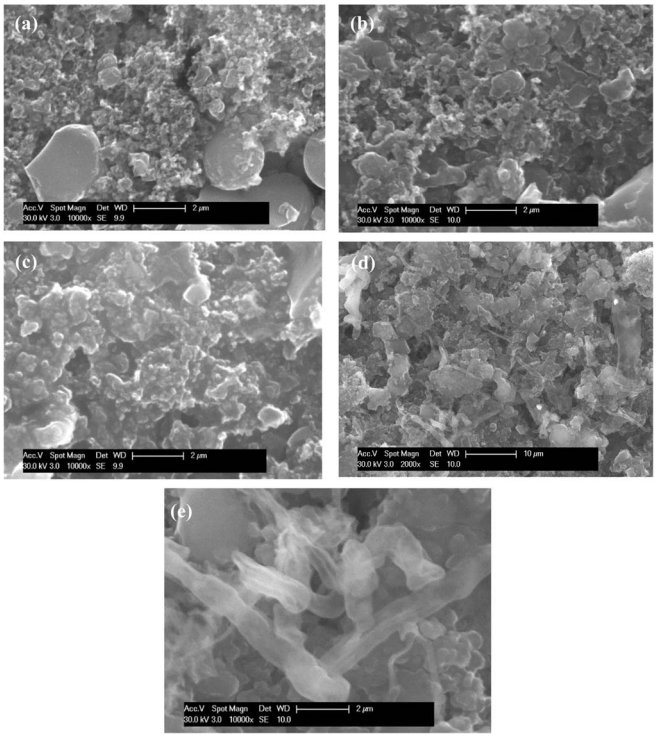

Figure 7. SEM images of pristine Si/C electrode (a) before cycling, (b) after cycling and non-prelithiated, (c) prelithiated at 0.5 V, (d) prelithiated at 0.1 V, and (e) appearance of lithium dendrites on the prelithiated at 0.1 V.

non- prelithiated Si/C – i.e. 86% vs 25%. Furthermore, differential capacity (dQ/dV) analysis shows that the cell with Si/C prelithiated at 0.1 V exhibited much less degradation due to a larger amount of available Li. However, Li deposition occurred in this cell, as shown in the three-electrode cell set-up. The electrode prelithiated at 0.5 V vs. Li/Li^+ showed no presence of Li dendrites, but it did not provide enough lithium. Prelithiation enables us to improve the electrochemical performance by (i) reducing the irreversible capacity of the negative electrode and (ii) providing a lithium reservoir to compensate for ongoing losses during cycling. However, controlling the degree of prelithiation is of great importance. The results from this study could be the basis for controlling the prelithiation process more precisely in future work which would be devoted to investigating different voltages of prelithiation in the potential range of 0.1–0.5 V vs. Li/Li^+ as well as applying chemical lithiation for comparison.

Acknowledgment

This work was financially supported by the Austrian Federal Ministry for Transport, Innovation and Technology (BMVIT).

Table I. Qualitative analysis of elemental mapping based on EDX analysis (% At).

Electrodes	C	Si	Cu	O	F	P
Pristine	92.37	7.17	0.5			
Non-prelithiated	79.69	3.72	0.53	13.25	2.42	0.4
Prelithiated at 0.5 V	71.21	3.39	0.47	16.34	6.98	1.61
Prelithiated at 0.1V	58.57	2.44	0.13	33.05	4.96	0.86

ORCID

Arlavinda Rezqita https://orcid.org/0000-0001-9101-3939
Jürgen Kahr https://orcid.org/0000-0001-8355-8533

References

1. S. R. Sivakkumar, J. Y. Nerkar, and A. G. Pandolfo, *Electrochim. Acta*, **55**, 3330 (2010).
2. M. N. Obrovac and L. Christensen, *Electrochem. Solid-State Lett.*, **7**, A93 (2004).
3. M. N. Obrovac and V. L. Chevrier, *Chem. Rev.*, **114**, 11444 (2014).
4. A. Rezqita, M. Sauer, A. Foelske, H. Kronberger, and A. Trifonova, *Electrochim. Acta*, **247**, 600 (2017).
5. K. Feng, M. Li, W. Liu, A. G. Kashkooli, X.-C. Xiao, C. Mei, and Z. Chen, *Small*, **14** (2018).
6. F. Holtstiege, P. Bärmann, R. Nölle, M. Winter, and T. Placke, *Batteries*, **4**, 4 (2018).
7. V. L. Chevrier, L. Liu, R. Wohl, A. Chandrasoma, J. A. Vega, K. W. Eberman, P. Stegmaier, and E. Figgemeier, *J. Electrochem. Soc.*, **165**, A1129 (2018).
8. R. Elazari, G. Salitra, G. Gershinsky, A. Garsuch, A. Panchenko, and D. Aurbach, *Electrochem. commun.*, **14**, 21 (2012).
9. K. Eom, J. T. Lee, M. Oschatz, F. Wu, S. Kaskel, G. Yushin, and T. F. Fuller, *Nat. Commun.*, **8**, 1 (2017).
10. A. Krause, S. Dörfler, M. Piwko, F. M. Wisser, T. Jaumann, E. Ahrens, L. Giebeler, H. Althues, S. Schädlich, J. Grothe, A. Jeffery, M. Grube, J. Brückner, J. Martin, J. Eckert, S. Kaskel, T. Mikolajick, and W. M. Weber, *Sci. Rep.*, **6**, 1 (2016).
11. Y. Yan, Y. X. Yin, S. Xin, J. Su, Y. G. Guo, and L. J. Wan, *Electrochim. Acta*, **91**, 58 (2013).
12. L. Fei, S. H. Yoo, R. A. R. Villamayor, B. P. Williams, S. Y. Gong, S. Park, K. Shin, and Y. L. Joo, *ACS Appl. Mater. Interfaces*, **9**, 9738 (2017).
13. H. J. Kim, S. Choi, S. J. Lee, M. W. Seo, J. G. Lee, E. Deniz, Y. J. Lee, E. K. Kim, and J. W. Choi, *Nano Lett.*, **16**, 282 (2016).
14. K. Min, K. Kim, C. Jung, S. W. Seo, Y. Y. Song, H. S. Lee, J. Shin, and E. Cho, *J. Power Sources*, **315**, 111 (2016).
15. H. Noh, S. Youn, C. Seung, and Y. Sun, **233**, 2 (2013).
16. M. Ender, A. Weber, and E. Ivers-TiffeÉe, *J. Electrochem. Soc.*, **159**, A128 (2012).
17. R. Jung, R. Morasch, P. Karayaylali, K. Phillips, F. Maglia, C. Stinner, Y. Shao-Horn, and H. A. Gasteiger, *J. Electrochem. Soc.*, **165**, A132 (2018).
18. M. Klett, J. A. Gilbert, S. E. Trask, B. J. Polzin, A. N. Jansen, D. W. Dees, and D. P. Abraham, *J. Electrochem. Soc.*, **163**, A875 (2016).
19. I. Bloom, L. K. Walker, J. K. Basco, D. P. Abraham, J. P. Christophersen, and C. D. Ho, *J. Power Sources*, **195**, 877 (2010).
20. M. Klett, J. A. Gilbert, K. Z. Pupek, S. E. Trask, and D. P. Abraham, *J. Electrochem. Soc.*, **164**, A6095 (2017).
21. S. M. Liang, F. Taubert, A. Kozlov, J. Seidel, F. Mertens, and R. Schmid-Fetzer, *Intermetallics*, **81**, 32 (2017).
22. M. Petzl, M. Kasper, and M. A. Danzer, *J. Power Sources*, **275**, 799 (2015).
23. N. Legrand, B. Knosp, P. Desprez, F. Lapicque, and S. Raël, *J. Power Sources*, **245**, 208 (2014).
24. P. Arora, M. Doyle, and R. E. White, *J. Electrochem. Soc.*, **146**, 3543 (1999).
25. T. Waldmann, B. I. Hogg, and M. Wohlfahrt-Mehrens, *J. Power Sources*, **384**, 107 (2018).
26. F. Ding, W. Xu, G. L. Graff, J. Zhang, M. L. Sushko, X. L. Chen, Y. Y. Shao, M. H. Engelhard, Z. M. Nie, J. Xiao, X. J. Liu, P. V. Sushko, J. Liu, and J. G. Zhang, *J Am Chem Soc*, **135**, 4450 (2013).
27. D. Aurbach, *J. Electrochem. Soc.*, **145**, 1421 (1998).